Catalysis Science & Technology

Accepted Manuscript

ROYAL SOCIETY OF CHEMISTRY

www.rsc.org/catalysis

Table of content

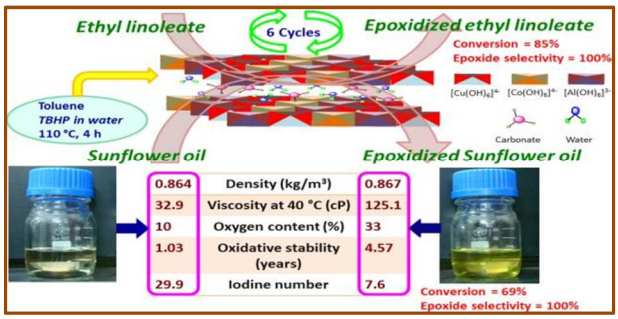

A scalable catalytic process for industrially important fatty epoxides is achieved by epoxidation of unsaturated fatty derivatives over recyclable CoCuAl-LDHs

Journal Name

RSCPublishing

ARTICLE

CoCuAl layered double hydroxides – Efficient solid catalysts for the preparation of industrially important fatty epoxides†

Cite this: DOI: 10.1039/x0xx00000x

Received 00th January 2012,
Accepted 00th January 2012

DOI: 10.1039/x0xx00000x

www.rsc.org/

Sivashunmugam Sankaranarayanan,[a,b] **Ankita Sharma**[a] and **Kannan Srinivasan**[a,b]

CoCuAl ternary layered double hydroxides (LDHs) with (Co+Cu)/Al atomic ratio of 3.0 with varying Co/Cu atomic ratios were synthesized by co-precipitation. Catalytic epoxidation of ethyl linoleate was carried out over these materials using aqueous *tert*-butyl hydroperoxide (70 wt.%) as oxidant. $Co_{30}Cu_{70}$Al-LDH (Co:Cu atomic ratio of 30:70) showed maximum conversion of 85% with 100% selectivity of epoxide at 110 °C in 4 h. Higher activity of this catalyst was attributed to synergism between cobalt and copper as inferred through physicochemical techniques. The catalyst was reusable for six times without significant loss. Study extended to vegetable oils (edible, non-edible and used cooking oils) showed 50-70% conversion with 100% selectivity. Comparison of activity between oils and fatty acid methyl esters (FAME) showed lesser activity for former probably due to hindered access. The process was successfully scaled-up (50 g) for sunflower oil and the physical properties were markedly varied for epoxidized oil suggests promise for industrial applications.

Introduction

Layered double hydroxides (LDHs; also referred as hydrotalcite-like (HT-like) materials) are well known materials as they find potential applications as multifunctional catalysts,[1] catalytic supports,[2] ion-exchangers,[3] polymer stabilizers,[4] photoactive materials[5] and in pharmaceuticals[6]. Structurally, they are similar to two-dimensional layered lattice structure of brucite ($Mg(OH)_2$, wherein partial substitution of bivalent metal ion (like Mg^{2+}) by trivalent ion, say Al^{3+} occurs and the resulting excess positive charge in the layers are compensated by anions (usually carbonate) for charge neutrality that occupy in the interlayers along with water molecules. The general formula of these materials are represented as $[M(II)_{1-x}M(III)_x(OH)_2]^{x+}$ $[A_{x/n}{}^{n-}]^{x-}.mH_2O$, where M(II) and M(III) are divalent and trivalent cations, A^{n-} is the interlayer anion and x can generally have the values between 0.20 and 0.40[7]. Owing to their flexible structural nature and ability to tune/obtain desired properties through facile synthetic/ modification processes, both as-synthesized LDHs and their modified forms are extensively studied as catalysts for various organic transformations.[8-13]

Vegetable oils and their fatty acid derivatives fall under the category of renewable resources gained increasing attention for the production of fuel/chemicals because of their surplus availability and biodegradability.[14] Introducing new functional groups in the vegetable oils/fatty derivatives provides huge industrial market opportunities through value-added products or as valuable intermediate and can be the best replacement for similar products derived through petroleum.[15] Due to the presence of unsaturation, long chain fatty derivatives show less oxidative stability and poor cold flow properties that makes them not suitable for fuel applications that can be circumvented by the conversion of olefinic group such as hydrogenation or epoxidation followed by ring opening.[16] Epoxidized vegetable oils are potential high temperature lubricants while their ring opened products can be used as low temperature lubricants.[17, 18] In addition, the presence of highly active oxirane ring makes long chain fatty epoxides as starting material for the preparation of polyurethane foams,[19] synthetic detergents,[20] stabilizers[21] and polymers[22]. Generally, epoxidized vegetable oils are produced by the well-known acid catalyzed Prileschajew reaction using organic acids along with hydrogen peroxide.[23, 24] Requirement of environmentally unfriendly strong mineral acid as catalyst, corrosion to equipments, non-selective products formation, separation difficulties, safety issues and generation of huge amount of residue makes this process unattractive.[25] Developing a process that uses environmentally benign heterogeneous catalysts is a best alternative to overcome these difficulties. Suarez et al. reported epoxidation of methyl oleate using commercial alumina as catalyst with low conversion of 33% in 6 h.[16] Titanium catalysts were reported extensively in the epoxidation of fatty acid derivatives with different oxidants such as *tert*-butyl hydroperoxide (TBHP) and hydrogen peroxide.[26, 27] Recently, acidic resins were reported as effective Prileschajew reaction catalyst for the epoxidation of Jatropha oil.[28] Studies were also made using molybdenum based catalysts for the epoxidation of different vegetable oils and biodiesel.[29-31] Although, enzyme catalysts showed excellent activity for the preparation of epoxidized corn oil,[32] owing to their high cost they are unattractive at this stage.

Developing low cost heterogeneous catalyst that renders high yields of epoxides for a range of fatty derivatives and vegetable oils is an exciting and industrially important task. Herein, successful synthesis of epoxidized ethyl linoleate and epoxidized vegetable oils in moderate to high yields is reported over a ternary CoCuAl LDH as environmentally benign low cost heterogeneous catalyst using TBHP (70 wt.% in water) as oxidant. To the best of our knowledge, this is the first report on epoxidation of linoleate and vegetable oils using LDHs as catalysts.

Results and discussion

Material characterization

The elemental chemical analysis and lattice parameters of the materials along with the calculated formula are given in the ESI Table S1. The Co/Cu and (Co+Cu)/Al ratios in the solids nearly matched well with the starting solutions and slight variation may be due to the incomplete precipitation of some of the cations.[33] In deriving the formula of the materials, carbonate content was calculated based on (Co+Cu)/Al ratio by assuming it as the only charge balancing interlayer anion. The water content was calculated from the TGA profiles considering the first weight loss before which both physically adsorbed and interlayer water molecules are removed upon heating. The powder X-ray diffraction (PXRD) patterns of the as-synthesized materials are shown in Fig. 1. All synthesized materials except $Co_{10}Cu_{90}$Al-LDH exhibited phase pure hydrotalcite-like structure (JCPDS: 41-1428) without any crystalline impurity phases while $Co_{10}Cu_{90}$Al-LDH showed copper oxide (CuO; tenorite (JCPDS: 00-045-0937)). The materials showed sharp and symmetric reflections at lower diffraction angles (peaks at 2θ = 11, 24 and 35° respectively) ascribed to the diffraction from the basal planes (003), (006) and (009). The broad asymmetric reflections at higher diffraction angles (peaks at 2θ = 38, 46 and 60° respectively) are ascribed by the diffraction from the planes (105), (108) and (110). As Cu content increased, the basal peaks became sharper and stronger which shows the increase in the crystallinity of the solids.[34]

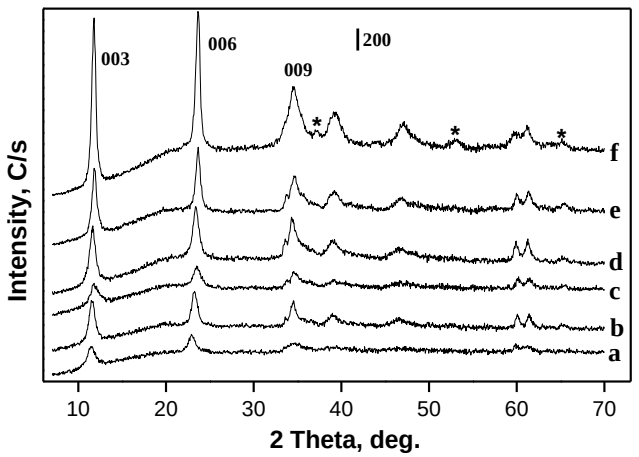

Fig. 1. PXRD patterns of (a) $Co_{100}Cu_0$Al-LDH, (b) $Co_{90}Cu_{10}$Al-LDH, (c) $Co_{70}Cu_{30}$Al-LDH, (d) $Co_{50}Cu_{50}$Al-LDH, (e) $Co_{30}Cu_{70}$Al-LDH, (f) $Co_{10}Cu_{90}$Al-LDH. *Copper oxide (CuO; Tenorite)

The lattice parameter 'a' which corresponds to M-M distance in the brucite-like layers and the lattice parameter 'c' which is three times the distance between the adjacent brucite like layers that is governed by the size of the interlayer anion and the columbic force of interaction between the interlayer anion and the layers are given in ESI Table S1. The lattice parameter 'a' increased with an increase in copper content due to higher octahedral ionic radii of Cu^{2+} (0.73 Å) than Co^{2+} (0.65 Å). Although (Cu+Co)/Al atomic ratio was nearly similar for all these materials, subtle variation 'c' parameter was noticed probably due to varied electrostatic interaction between layers and the interlayer. The Fourier transformed infrared (FT-IR) spectra of all the as-synthesized materials (Fig. 2; solid line) showed a broad absorption band around 3500-3600 cm^{-1} attributed to the hydrogen bonded stretching vibration of the -OH group in the brucite like layer. Band observed at 1650 cm^{-1} corresponds to the bending vibration of water molecules. IR active absorption bands observed at 1350-1380 cm^{-1} (ν_3) , 850-870 cm^{-1} (ν_2) and 670-690 cm^{-1} (ν_4) corresponds to asymmetric, out-of- plane and in-plane bending vibrations respectively of carbonate anion, characterized by its D_{3h} symmetry. These bands shifted slightly towards higher wave number with an increase in Cu content.

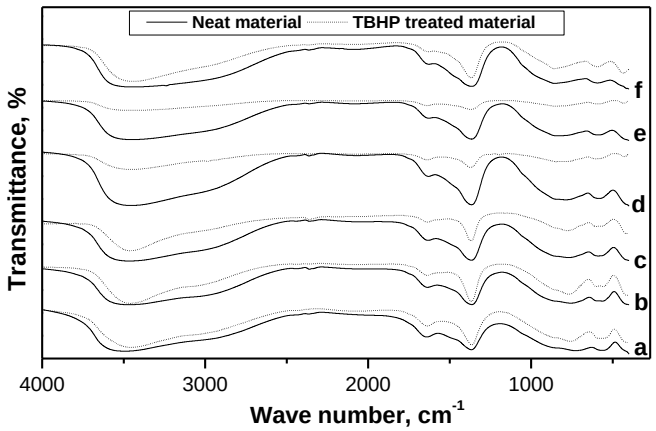

Fig. 2. FT-IR spectra of (a) $Co_{100}Cu_0$Al-LDH, (b) $Co_{90}Cu_{10}$Al-LDH, (c) $Co_{70}Cu_{30}$Al-LDH, (d) $Co_{50}Cu_{50}$Al-LDH, (e) $Co_{30}Cu_{70}$Al-LDH, (f) $Co_{10}Cu_{90}$Al-LDH

TG-DTG (differential thermogravimetric) profiles of all the as-synthesized LDH materials are shown in ESI Fig. S1. $Co_{100}Cu_0$Al-LDH showed two different weight losses around 200 and 300 °C. The first weight loss between 100-200 °C is due to the removal of physically adsorbed water molecules from the lattice. The second weight loss between 220-300 °C is due to dehydroxylation and decarbonation leading to the structural collapse of the materials. As Cu content increased, the first loss shifted to lower temperature region along with the disappearance of second weight loss. This suggests the occurrence of structural loss at lower temperature for higher Cu containing materials. Scanning electron microscopy (SEM) images of the samples exhibited platelet like morphology agglomerated to spongy like structure which is common in HT-like materials.[35] $Co_{10}Cu_{90}$Al-LDH showed two different morphologies may be due to the formation of separate copper oxide particles (ESI Fig. S2), as supported earlier by PXRD studies.

UV-vis spectra of the as-synthesized materials are given in ESI Fig. S3. High intense peaks observed in 200-300 nm (UV region) for all the LDH materials are ascribed for charge transfer processes. $Co_{100}Cu_0$Al-LDH showed two broad adsorption maxima around 350 and 530 nm which are characteristic for Co^{2+} octahedral species and are associated with the transitions $^4T_{1g}(F) \rightarrow {}^4T_{1g}(P)$ and $^4A_2(F) \rightarrow {}^4T1(P)$ respectively. As the Cu content increased, the intensity of the above-mentioned transition decreased with an appearance of new broad absorption peak around 750 nm ($^2E_g \rightarrow {}^2T_{2g}$), characteristic of Cu^{2+} in octahedral coordination with Jahn-Teller distortion.[34]

Catalytic activity of the as-synthesized materials

In the preliminary studies, all the as-synthesized materials were tested for the epoxidation of ethyl linoleate using 70 wt.% aqueous TBHP as oxidant and the results are given in Table 1. Blank reaction (only ethyl linoleate and toluene) without using catalyst and oxidant at 110 °C showed very low conversion of ethyl linoleate (5%) and indicated no molecular changes suggests the stability of the reactant under the reaction conditions (in turn supports the calculation for determining conversion of ethyl linoleate). An increase in the Cu content increased the conversion with nearly similar epoxide selectivity up to 70% substitution of copper ($Co_{30}Cu_{70}$Al-LDH). A further increase, however, resulted in a decrease in the conversion as well as selectivity of epoxides due to the formation of hydroxylated products. Such formation of hydroxylated products are likely due the presence of water molecules (from aqueous TBHP) present in the reaction mixture. The decrease in the activity of the catalyst having higher copper content could probably due to the presence of copper oxide. In order to discern this, catalytic activity of CuO (equivalent % Cu in $Co_{30}Cu_{70}$Al-LDH catalyst) was carried out that showed less selectivity of epoxide (66%) augments the presence of CuO is unfavorable for this reaction. Furthermore, the synthesis of Co_0Cu_{100}Al-LDH ended in failure and the catalytic activity of this material showed epoxides along with the formation of large amount of unidentified by-products (based on the appearance of new peaks in ^{1}H NMR). From these studies it can be concluded that co-presence of copper along with cobalt in the LDH matrix at optimal concentration is beneficial for the epoxidation reaction rendering high selectivity of epoxides. Reaction performed in the absence of catalyst (with ethyl linoleate, toluene and TBHP) and without oxidant (with ethyl linoleate, toluene and catalyst) gave 38% and 21% conversion respectively with 100% epoxide selectivity (Table 1; Entry No.10&11) and these results indicate the necessity of both catalyst and the oxidant to obtain high yields of epoxides. Catalytic activity of $Co_{30}Cu_{70}$Al-LDH at room temperature showed 44% conversion with 100% epoxide selectivity and the blank reaction at room temperature gave only 25% conversion with similar selectivity. Though stoichiometric epoxide selectivity was achieved in both the above mentioned cases (Table 1; Entry No.12&13), diepoxide selectivity was very low (in other words ethyl linoleate predominantly undergo monoepoxidation) suggests the necessity of higher temperature for the occurrence of subsequent epoxidation of monoepoxides to diepoxide. In literature, no specific application has been discussed for the mono and diepoxides of fatty derivatives and both may have different application because of varying physical properties.

Interaction of TBHP with the catalyst is expected to play an important role in this reaction and to find this FT-IR studies were done for the TBHP treated catalysts (Fig. 2; dotted line). As the Cu content increased, the intensity of hydroxyl adsorption band (-OH) decreased up till for $Co_{30}Cu_{70}$Al-LDH (Fig. 2, e). This suggests the coordination of TBHP with the surface hydroxyl groups which in turn possibly involves in promoting the epoxidation reaction. Though, $Co_{50}Cu_{50}$Al-LDH and $Co_{30}Cu_{70}$Al-LDH showed a similar decrease in the intensity of this band, higher activity of the latter might be due to its higher Cu content. Although $Co_{10}Cu_{90}$Al-LDH has higher Cu content than $Co_{30}Cu_{70}$Al-LDH, the interaction between the catalyst and TBHP was poor (Fig. 2, f). Specific surface areas of these materials (Table 1) were low in the range of 35-45 m^2/g except for $Co_{50}Cu_{50}$Al-LDH which showed 70 m^2/g. Though, the surface area of the latter material is high, its catalytic activity was lesser than the most active $Co_{30}Cu_{70}$Al-LDH suggests non-influence of the surface area on reactivity of these materials under studied conditions. Owing to the high activity exhibited, $Co_{30}Cu_{70}$Al-LDH catalyst was chosen as the optimized catalyst and studied further by varying parameters with an endeavor to improve the yield.

Hammett indicator studies

Hammett indicator measurement is the one of the widely accepted methods for the determination of acidic as well as basic strength of the catalysts.[36] Hammett indicator studies were done for all the catalysts using different indicators. All catalysts showed similar acidic strength range (-5.6< H_ <-8.2) while CuO exhibited lesser. Interestingly, the same trend was observed for basic strength also in which CuO showed lesser basic strength range than other catalysts (8.2< H_ <10.1). Though, this study did not show any relatable results in terms of variation in the activity upon changing Cu/Co atomic composition, it can be safely concluded that besides acidity/basicity, some other factors may play main role in this reaction. These findings then prompted to find out the variation in the reducibility of the LDH materials which might have an influence on the catalytic activity.

Table 1 Catalytic activity of the as-synthesized CoCuAl LDHs for ethyl linoleate epoxidation along with surface properties

Entry No.	Catalyst[a]	Conv. (%)	Selectivity of epoxide (%)	Selectivity (%)		Surface Property	
				Monoepoxide	Diepoxide	Surface area (m^2/g)	Pore volume (cm^3/g)
1.	Blank[b]	5	100	71	29	-	-
2.	$Co_{100}Cu_0$Al-LDH	65	100	39	61	44	0.08
3.	$Co_{90}Cu_{10}$Al-LDH	69	100	20	80	-	-
4.	$Co_{70}Cu_{30}$Al-LDH	77	100	22	78	-	-
5.	$Co_{50}Cu_{50}$Al-LDH	76	100	15	85	70	0.16
6.	$Co_{30}Cu_{70}$Al-LDH	85	100	13	87	35	0.06
7.	$Co_{10}Cu_{90}$Al-LDH	80	78	15	85	34	0.06
8.	Co_0Cu_{100}Al-LDH[c]	73	67	12	88	-	-
9.	CuO[d]	72	66	16	84	-	-
10.	Without catalyst	38	100	85	15	-	-
11.	$Co_{30}Cu_{70}$Al-LDH[e]	21	100	89	11	-	-
12.	$Co_{30}Cu_{70}$Al-LDH[f]	44	100	71	29	-	-
13.	Without catalyst[f]	25	100	83	17	-	-

[a]TBHP:Ethyl linoleate = 3:1 mole ratio, Toluene = 2 ml, Temp. = 110 °C, Catalyst = 5 wt.% w.r.t. ethyl linoleate, Time = 4 h; [b]only substrate; [c]no phase pure LDH was present; [d]equivalent to % Cu in $Co_{30}Cu_{70}$Al-LDH catalyst; [e]without oxidant; [f]room temperature

Journal Name RSCPublishing

ARTICLE

Temperature programmed reduction studies

Temperature programmed reduction (TPR) is a technique used to get an idea about the reducibility of materials. In the TPR studies of CoCuAl-LDHs, the divalent cations Co and Cu are reduced to their metallic state while the trivalent cation ($A1^{3+}$) is unaffected in the temperature range studied. CuO is used to calibrate the TPR instrument and the TPR profiles of as-synthesized CoCuAl-LDHs are given in Fig. 3. For, $Co_{100}Cu_0$Al-LDH a broad H_2 consumption peak was observed around 530 °C which was completely absent with the addition of copper in the material. Copper containing LDH materials, showed two components reduction peak around 220-360 °C with broad peaks at low copper content and the peak splitting become clearly visible and gets sharpened with an increase in Cu content. These results suggest substituting Cu^{2+} for Co^{2+} in LDH system facilities reduction of latter and thereby influencing the redox characteristics of these materials. This could be due to spill-over effects as discussed earlier for CuNiAl LDH systems.[37]

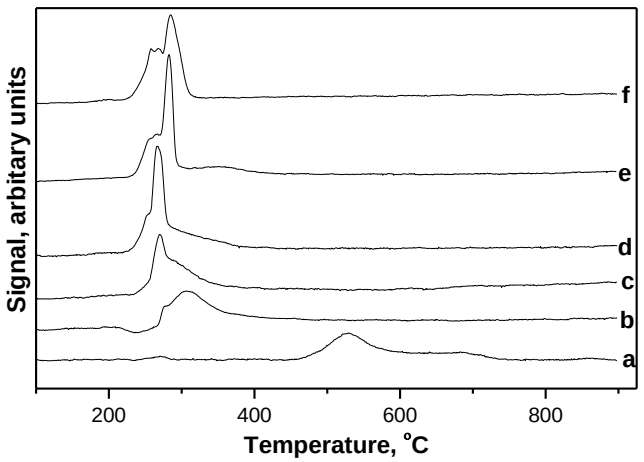

Fig. 3. TPR profiles of (a) $Co_{100}Cu_0$Al-LDH, (b) $Co_{90}Cu_{10}$Al-LDH, (c) $Co_{70}Cu_{30}$Al-LDH, (d) $Co_{50}Cu_{50}$Al-LDH, (e) $Co_{30}Cu_{70}$Al-LDH, (f) $Co_{10}Cu_{90}$Al-LDH

H_2 consumption and H_2/metal ratios derived from TPR for the materials are given in Table 2. Among the catalysts, $Co_{100}Cu_0$Al-LDH showed lesser value for H_2/metal ratio suggests incomplete metal (here Co^{2+}) reduction for this catalyst as witnessed by the presence of broad high temperature reduction peaks observed above 600 °C. However, all the other catalysts showed an expected H_2/metal ratio of around 1.0 and the deviations are within the instrumental error. Although, TPR results showed significant variations in the reduction behavior of metal ions (here Co and Cu) upon changing the concentration of copper in CoCuAl-LDH, in other words, noteworthy modifications in the redox properties of these materials that would influence oxidation/reduction reactions, no satisfactory explanation could be discerned either based on the temperature of reduction or from the reduction profile for the relatively high activity observed for $Co_{30}Cu_{70}$Al-LDH. Efforts were then laid on studying surface characteristics of these samples.

Table 2 TPR results of CoCuAl-LDH materials

Catalyst	TPR studies	
	H_2 consumption (μ mol/g)	H_2/Metal (Molar ratio)
$Co_{100}Cu_0$Al-LDH	5948	0.78
$Co_{90}Cu_{10}$Al-LDH	7435	1.08
$Co_{70}Cu_{30}$Al-LDH	7254	1.00
$Co_{50}Cu_{50}$Al-LDH	7615	1.07
$Co_{30}Cu_{70}$Al-LDH	7435	1.06
$Co_{10}Cu_{90}$Al-LDH	7348	1.06
CuO	12709	1.00

X-ray photoelectron spectroscopy studies

X-ray photoelectron spectroscopy (XPS) studies were carried out for some of the catalysts and O 1s, Co 2p and Cu 2p XP spectra are given in Fig. S4 and surface elemental composition, binding energies, full-width at half maximum (FWHM) and intensity ratios calculated are given in Table S2. C 1s spectra showed a peak at binding energy around 289.6 eV confirms the presence of carbonate in LDH materials.[38] Binding energy observed around 529-530 eV for O 1s region corresponds to the characteristic hydroxyl environment in LDH materials.[39] All materials showed Al 2p binding energy around 74 eV, substantiating the presence of Al^{3+}. The Cu $2p_{3/2}$ region showed binding energies around 935 eV characteristic for Cu^{2+}.[35] The presence of Cu^{2+} can also be confirmed by the presence of intense satellite peak around 942 eV in all the samples.[40] The intensity ratio between the main peaks (Im) and the satellite peaks (Is) for $Co_{50}Cu_{50}$Al-LDH was 0.44 while 0.52 for $Co_{10}Cu_{90}$Al-LDH suggests variable charge density around copper ions as its concentration was varied in the samples. Further these values for LDHs having higher Cu content were nearly similar to CuO[41], as supported earlier by PXRD that showed segregation of CuO for these samples. The Co $2p_{3/2}$ region showed binding energies around 781 eV which are characteristic for cobalt in +2 oxidation state.[38] Binding energy difference between the main peaks of Co $2p_{3/2}$ and Co $2P_{1/2}$ was around 16 eV for these materials further confirms the oxidation state cobalt. The FWHM values for Co 2p region for the samples were in the range 1.8-2.7 eV that showed enhanced broadening (for both main and satellite peaks) with increasing Cu content.

The surface composition of Co/Cu showed acceptable deviation compared to bulk composition determined using ICP-OES studies. These values were on the higher side suggests surface enrichment of cobalt. However, a significant variation in (Cu+Co)/Al atomic ratio was noted between bulk and surface composition suggests surface enrichment of transition metal ions compared to Al^{3+} probably due to their low surface free energies. The ratio increased with an increase in copper content till an optimum level and decreased thereafter. The active catalyst ($Co_{30}Cu_{70}$Al-LDH) showed highest surface (Cu+Co)/Al atomic ratio of 12.2. To surmise, XPS studies showed that nearly similar binding energies for all catalysts for the elements screened suggests the variation could not possibly

be due to variation in the electronic environment around the active metal ions, here Co^{2+} and Cu^{2+} to enable the epoxidation reaction. However, variation in the surface atomic composition could be correlated to a reasonable extent on the activity trend observed.

Parametric variation studies

Catalyst amount variation studies (ESI Fig. S5) showed an increase conversion with an increase in the catalyst amount up to 3 wt.%; thereafter conversion remained almost same. Diepoxide formation was favorable at higher catalyst amount and 3 wt.% catalyst amount with respect to substrate was optimized for further studies. Time variation studies were done and the results are given in ESI Table S3. Conversion and selectivity of the reaction increase with an increase in reaction time up to 4 h and reached a maximum conversion of 84% with 100% epoxide selectivity. However, with a further increase in time lead to formation of alcohols through ring opening of epoxides. Hydrotalcites are also reported as good catalysts for the ring opening of fatty epoxides.[42] ^{1}H NMR spectra of time variation studies showed a decrease in the intensity and area of the product peaks (2.9 and 3.1 ppm) after 4 h and were completely vanished at 10 h (ESI Fig. S6). This shows the formation of unwanted products due to the consecutive reactions. Reaction temperature variation results are given in ESI Table S4 which indicated that temperature plays a main role in epoxidation reaction. Increase in temperature enhanced the conversion as well as improved the selectivity of diepoxide up to 110 °C and remained same thereafter and this temperature was chosen as optimum for further studies. Oxidant:substrate mole ratio variation studies revealed that an increase in the oxidant amount increased the conversion as well as epoxide selectivity (ESI Fig. S7). A maximum conversion was obtained at oxidant:substrate mole ratio of 3:1 and a further increase in the ratio did not show any significant variation in the conversion. A higher amount of oxidant lead to formation of ring opened product in trace amount as evidenced by the decrease in the selectivity of diepoxide. Although, only 1.63 equivalents of unsaturated bonds (calculated from the composition of ethyl linoleate) are available in ethyl linoleate, 3 equivalent of oxidant was needed to obtain high conversion.

In order to find out the mass transfer effects, reactions were carried out with variable stirring speed from 100-1100 rpm under the optimized reaction conditions and the results are given in ESI Table S5. Reaction conducted by stirring at 300-1100 rpm showed nearly similar conversion and yield of epoxides suggest no mass transfer effects beyond 300 rpm for this reaction. Other oxidants such as H_2O_2 (30 wt.% in water), air and oxygen were also screened as oxidant source for the epoxidation of ethyl linoleate. Air and oxygen gave 48 and 54% conversion respectively while H_2O_2 gave 19% only (ESI Table S6, Entry No.1-3). Though moderate conversions were achieved with air/oxygen, TBHP is the best oxidizing agent for this reaction under our optimized reaction conditions. In order to further increase the conversion of ethyl linoleate, reactions were carried out using TBHP as oxidant along with N_2 (or) O_2 atmosphere/ bubbling. No variation in the conversion was seen suggesting non-influence of reaction atmosphere (ESI Table S6, Entry No.4-7). MALDI-TOF analysis was done for epoxidized ethyl linoleate (for the entire reaction mixture obtained under the optimized reaction conditions given in ESI Table S4 for the data of 1100 rpm) and the mass fragmentation patterns are given in ESI Fig. S8. Though the expected m/z value for epoxidized ethyl linoleate is 340, high intense signal was observed at 379.05 probably due to $[M+K]^+$ formation. A small intense peak was also observed at 362.02 which may be due to the formation of $[M+Na]^+$ ions. This result further corroborates the successful epoxidation of ethyl linoleate over this catalyst.

Calcination temperature variation studies

Calcination of LDHs lead to the decomposition of layered structure and results in homogeneous mixed metal oxides predominately with Lewis basic character (although co-presence of Brønsted sites is governed by calcination temperature and nature of metal ions in the lattice) which are generally more active catalysts than as-synthesized materials for many base catalyzed organic transformations.[13] To maximize the conversion of ethyl linoleate and also for scientific curiosity, the optimized catalyst $Co_{30}Cu_{70}$Al-LDH was calcined at different temperatures and studied for epoxidation reaction. The PXRD pattern of the 300 °C calcined material showed conversion of LDH into amorphous phase whereas the sample calcined at 500 and 700 °C (ESI Fig. S9) showed spinel-like phase (it is very difficult to ascertain the composition of the spinel due to subtle variation in lattice parameters for many possible forms or their combinations namely Co_3O_4 (JCPDS:00-043-1003), Co_2AlO_4 (JCPDS:00-038-0814), $CuAl_2O_4$ (JCPDS:00-033-0448), $CoAl_2O_4$ (JCPDS:00-0303-0896), $(Cu_{0.3}Co_{0.7})Co_2O_4$ (JCPDS:00-025-0270), $Cu_{0.76}Co_{2.24}O_4$ (JCPDS: 00-036-1189) and $Cu_{0.92}Co_{2.08}O_4$ (JCPDS:00-037-0878) along with tenorite (CuO, JCPDS: 00-045-0937). The FT-IR spectra of calcined materials showed the absence of bands at 1350-1380 cm^{-1} and 1640 cm^{-1} confirms the structural decomposition (ESI Fig. S10).

The textural properties and catalytic activity of the calcined materials are shown in ESI Table S7. The results indicated that those materials calcined at 300 and 500 °C that have similar surface area and pore volume showed >80% of conversion with selectively diepoxides whereas 700 °C calcined material gave 65% conversion. The lesser conversion of this sample may probably be due to the presence of CuO phase and lesser surface area (50% decrease in the surface area than 300 and 500 °C calcined materials) of the material. From these studies it could be inferred that compared to as-synthesized catalysts, calcined materials are useful for selective formation of diepoxides from ethyl linoleate. Reusability studies of $Co_{30}Cu_{70}$Al-$CLDH_{300}$ showed successful recycling up to three cycles without any significant loss in its activity (ESI Table S8). Even though calcined material showed good activity and reusability for this reaction, the conversion was nearly similar to that of as-synthesized material. In view of energy needed for calcination and since the enhancement in the yield of epoxide was not significant, as-synthesized $Co_{30}Cu_{70}$Al-LDH material was considered as optimized catalyst for this reaction (compared to its calcined form) for further studies.

Reaction in presence of oleate/*tert*-butanol species

Parametric variation studies revealed that even after optimizing the reaction conditions the conversion of ethyl linoleate did not go beyond 85% that suggest there might be some factors that may limit in enhancing the conversion further. It was presumed that oleate species in the stock solution of ethyl linoleate (or) *tert*-butanol from aqueous TBHP might hinder in obtaining higher conversion of linoleate. In order to verify, epoxidation reaction was performed with the deliberate addition of methyl oleate/*tert*-butanol to the reaction system (ESI Fig. S11 & S12). An increase in the amount of oleate decreased the conversion and showed 70% conversion in presence of 25 wt.% of oleate, clearly indicates its inhibition effect on the conversion of ethyl linoleate under the optimized

conditions. Under these conditions, methyl oleate gave only 59% conversion with 60% epoxide selectivity. These results suggest that compare to oleate species, linoleate species are more prone to epoxidation reaction over these materials and it can be concluded that higher selectivity of diepoxide might be due the promoting effect of formed monoepoxides to diepoxide. On the contrary, the conversion of ethyl linoleate was similar under optimized condition when 50 wt.% of *tert*-butanol was deliberately added suggests even larger amount of aqueous layer did not influence the progress of the reaction, as is known that *tert*-butanol can acts as a phase transfer agent thereby facilitating the progress of the reaction.

Catalyst stability and reusability studies

To check the stability of the catalyst, an optimized amount of $Co_{30}Cu_{70}$Al-LDH catalyst was stirred in 2 ml of toluene at 110 ° C for 1 h. After recovering the catalyst, the supernatant solution was mixed with 1g of ethyl linoleate and appropriate amount of TBHP was added and kept at 110 ° C for 4 h to assess homogeneous contribution, if any. The supernatant solution showed a conversion value (40%) similar to that of the reaction in the absence of catalyst (Table 1; Entry No.10). This result supports the stable nature of the catalyst with very minimal leaching (ICP-OES showed leaching of 0.8% for Co, 2.5% for Cu and 0.4% for Al) and with negligible homogeneous contribution under the reaction conditions. To further validate, hot filtration leaching test was carried out wherein the catalyst was removed at 0.5 h under hot conditions and the reaction was allowed to continue for 4 h. A conversion of 63% was observed in 4 h for the catalyst-removed filtrate while 84% was observed in the presence of catalyst. This further confirms the insignificant contribution of leached metal ions (small variation could be due to influence of time by the oxidant present), in other words, corroborates negligible homogeneous contribution under the reaction conditions.

For reusability/recycle studies, after the reaction the catalyst ($Co_{30}Cu_{70}$Al-LDH) was separated from the reaction mixture by centrifugation and washed well with toluene to remove organics adhered on the catalyst surface and dried in an oven at 100 ° C for 1 h and this procedure was repeated before every cycle. Reusability of the catalyst was assessed under the optimized reaction conditions (Fig. 4).

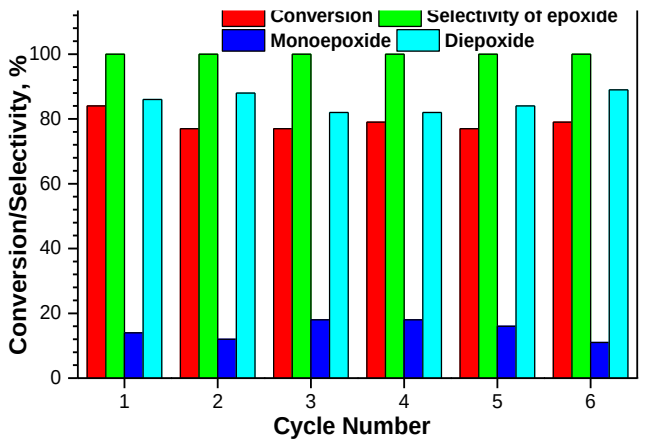

Fig. 4. Reusability studies. TBHP:Ethyl linoleate = 3:1 mole ratio, Catalyst = 3 wt.% w.r.t. ethyl linoleate, Toluene = 2 ml, Temp. = 110 °C, Time = 4 h.

The catalyst can be recycled up to six cycles without any loss in activity. Though, nearly similar conversion and selectivities were maintained, the product mixture however turned slightly viscous after sixth cycle for which the reasons are not clear. PXRD patterns of three times and six times used catalysts were similar as that of freshly prepared catalyst (ESI Fig. S13). However, FT-IR of three times and six times used catalysts showed the formation of new bands around 1750 (C=O stretching of ester) and 2936 cm^{-1} (C=H stretching of alkane) probably arising from adherence of organic moieties on the catalyst surface (ESI Fig. S14).

To ascertain further, XPS studies were carried out for used $Co_{30}Cu_{70}$Al-LDH catalyst and compared with fresh $Co_{30}Cu_{70}$Al-LDH catalyst (ESI Fig. S15). A significant surface enrichment of carbon (28 at.%) and reversal in the intensity ratio of carbonate carbon with that of organic carbon (C-H and C-C; B.E. ~285 eV) was revealed for the used catalyst corroborating the adherence of organic molecules on the surface of the catalyst that supported the observations of FT-IR. No significant change in the binding energies for both cobalt and copper was observed between the fresh and used $Co_{30}Cu_{70}$Al-LDH catalysts (Table 3). Although the actual surface concentration of both Co and Cu ions decreased for the used catalyst in comparison with that of fresh catalyst, the Co/Cu ratio was similar, suggests invariance in the surface atomic composition during the reaction. The lesser value could possibly be due to presence of organic moieties on the surface of the catalyst. The variation in (Co+Cu)/Al atomic ratio between fresh (12.2) and used catalyst (8.3) could possibly due to leaching of Al from the catalyst surface. In addition, the intensity ratios and FWHM between satellite and main peaks for both Co and Cu were nearly similar for fresh (I_s/I_m and FWHM for Co is 0.47 and 2.7 eV; Cu is 0.5 and 3.2 eV) and used (I_s/I_m and FWHM for Co is 0.51 and 2.7 eV; Cu is 0.5 and 3.6 eV) catalysts indicates no significant variation in the oxidation state and coordination environment.

Table 3 Surface atomic composition, binding energies, FWHM and intensity ratios of main and satellite peaks obtained through XPS studies for fresh and used $Co_{30}Cu_{70}$Al-LDH catalyst

$Co_{30}Cu_{70}$Al-LDH catalyst		Fresh	Used
Surface composition (atom%)[a]	**Co**	10.4	7.1
	Cu	14.0	9.5
	O	62.8	53.3
	C	10.0	28.0
	Al	2.0	2.0
	Co/Cu	0.7	0.7
	(Co+Cu)/Al	12.2	8.3
Binding energy (FWHM) eV	**Co 2p**	781.2 (2.7)	781.1 (2.7)
	Cu 2p	935.0 (3.2)	934.8 (3.6)
I_s/I_m	**Cu**	0.50	0.5
	Co	0.47	0.51

[a]Values rounded

Epoxidation of different vegetable oils

For further increasing the scope and validation of the reaction, epoxidation reaction was extended to various vegetable oils comprising edible, non-edible and used cooking oils. TBHP:oil mole ratio, conversion and selectivities along with iodine number of both reactants and products are given in Table 4. Non-catalytic and catalytic epoxidation of sunflower

Journal Name RSCPublishing

ARTICLE

Table 4 Epoxidation of different vegetable oils[a]

Entry No.	Name of the oil/reactant	TBHP: Oil (mole ratio)	Conv. (%)	Selectivity of epoxide (%)	Selectivity (%)		Iodine number (IV)[43]	
					Monoepoxide	Diepoxide	Oil[g]	Epoxide[g]
1.	Sunflower oil[b]	8.8:1	36	100	69	31	29.9	14.8
2.	Sunflower oil	8.8:1	69	100	10	90	29.9	7.6
3.	Sunflower oil	12.6:1	75	85	4	96	29.9	6.4
4.	Groundnut oil	7.7:1	60	100	22	88	26.5	8.2
5.	Gingelly oil	7.6:1	59	100	10	91	28.2	8.7
6.	Soyabean oil	7.6:1	69	100	12	88	37.3	9.3
7.	Cottonseed oil	7.9:1	64	100	14	86	27.0	7.0
8.	Corn oil	7.7:1	69	100	3	98	31.3	8.1
9.	Rice bran oil	7.7:1	60	100	18	82	25.3	6.8
10.	Jatropha curcus oil	7.2:1	70	100	44	56	26.8	7.8
11.	Pinnai oil	7.7:1	63	100	30	70	20.4	4.9
12.	Karingatta oil	8.1:1	67	100	26	74	29.4	7.9
13.	Castor oil	7.9:1	40	100	98	2	11.4	3.6
14.	Once cooked (sunflower) oil	7.1:1	68	100	15	85	38.0	9.8
15.	Doubly cooked (sunflower) oil	6.2:1	74	100	5	95	45.4	10.1
16.	Waste cooked (cottonseed) oil	6.8:1	75	100	14	86	27.3	5.7
17.	Sunflower FAME	2.9:1	78	100	6	94	-	-
18.	Sunflower FAME[c]	3.7:1	78	100	19	81	-	-
19.	Ethyl linoleate[d]	3.0:1	67	100	18	82	-	-
20.	Sunflower oil[e]	8.8:1	76	100	4	96	29.9	6.5
21.	Sunflower oil[f]	8:1	83	100	20	80	29.9	6.1
22.	Sunflower oil[e,f]	8:1	85	100	19	81	29.9	6.0

[a]Substrate = 1 g, TBHP = 1.4 ml, Toluene = 2 ml, Catalyst = 3 wt.% w.r.t. substrate, Temp. = 110 ºC, Time = 4 h; [b]without catalyst; [c]TBHP = 1.75 ml; [d]Reaction in presence of glycerol (Ethyl linoleate.:glycerol = 3:1 mole ratio); [e]antioxidant extracted oil; [f]TBHP in decane as oxidant; [g]Based on ^{1}H NMR analysis

oil gave 36 and 69% conversion respectively with 100% selectivity of epoxides (Table 4; Entry No.1&2) indicated the necessity of the catalyst for this reaction. Increase in the TBHP amount gave higher conversion (75%) but reduced the selectivity of epoxide to 85% analogous to the result observed for ethyl linoleate epoxidation (Table 4; Entry No.3). Edible oils such as groundnut, gingelly, soybean, cottonseed, corn and rice bran oil also gave conversion in the range of 60-70% with 100% epoxide selectivity and in all the cases the diepoxide selectivity are >80% (Table 4; Entry No.4-9).

Jatropha oil gave 70% conversion with 100% selectivity of epoxide (Table 4; Entry No.10) and the distribution of mono and diepoxides were 44/66%. In this oil, the product mixture turned green possibly due to the leaching of copper owing to the presence of high amounts of free fatty acid (ICP-OES analysis showed ~2 wt% of Cu leaching in the oil layer). Pinnai oil gave 63% conversion with the mono and diepoxide selectivities of 30 and 70 % respectively (Table 4; Entry No.11) while karingatta oil (Table 4; Entry No.12) that had similar fatty composition as pinnai oil showed similar conversion and selectivity (67% conversion with mono and diepoxide selectivities of 26 and 74%). Castor oil predominantly has functionalized fatty acid called ricinoleic acid (18:1) that can only forms monoepoxide owing to the presence of one unsaturated centre. Epoxidation of castor oil gave 40% conversion with 98% monoepoxide selectivity (Table 4; Entry No.13) and the likely reason for the lesser conversion may be due to the formation of hydrogen bonding between the hydroxyl groups in the fatty chain with water molecules present in the system which makes the fatty derivative more hydrophilic.

Further, epoxidation of used cooking oil under the optimized reaction conditions showed similar conversion like other oil sources with 100% epoxide selectivity (Table 4; Entry No.14-16). These results suggest that non-edible oils as well as used cooking oils can also be efficiently used for the preparation of fatty epoxides than by using edible oils thereby averting food vs fuel issues. FAME produced from sunflower oil (sunflower biodiesel) showed 78% conversion with 100%

selectivity which is comparatively higher than neat sunflower oil (Table 4; Entry No.17). Glyceryl moiety in the form of triglycerides is the only structural difference between sunflower oil and sunflower FAME and hence this may have some influence on the progress of the reaction. To prove, ethyl linoleate epoxidation was carried out in the presence of deliberately added glycerol (Ethyl linoleate:glycerol = 3:1 mole ratio, same as in triglycerides). The conversion was similar as that of sunflower oil (Table 4; Entry No.19). This suggests that the presence of this moiety in the system hinders the progress of the reaction by reducing the accessibility of TBHP towards the unsaturated centres while in FAME/ethyl linoleate, TBHP can approach the unsaturated centres easily from any direction due to its easy mobility and hence showed higher conversion (ESI Fig. S16). In addition, the highly viscous glycerol moiety may block the active sites on the catalyst surface and thus result in lesser conversion in vegetable oils than FAME/ethyl linoleate.

Interestingly, an increase in the TBHP amount beyond the optimized amount gave same conversion but with an increase in the monoepoxide selectivity for sunflower FAMEs (Table 4; Entry No.18) suggests the occurrence of ring opening of diepoxide to hydroxylated/other products. It is worth mentioning here that in the case of FAMEs epoxidation, the error in the selectivity value is ± 2%, which is comparatively lesser than that of oils (±5%). In the case of sunflower oil epoxidation, maximum conversion achieved was around 70% with 100% selectivity of epoxides and it was comparatively lesser than ethyl linoleate under the optimized conditions. Antioxidant addition is the one of the unit processes during refining of vegetable oils and the presence of such compounds could be detrimental for this reaction by suppressing the activity of the TBHP. It is worth noting here that waste cooked oils gave higher conversion than neat sunflower oil and this may probably due to the removal of antioxidants during cooking process. To verify further, sunflower oil used for this reaction was extracted with methanol to remove any commonly used antioxidants (such as *tert*-butylhydroquinone) and was studied for epoxidation. The conversion increased to 76% with 100% epoxide selectivity (Table 4; Entry No.20). In addition, when the reactions were carried out using TBHP in decane as oxidant, the conversion increased further to 83 and 85% for sunflower oil and antioxidant extracted sunflower oil respectively (Table 4; Entry No.21&22).

Comparison with different catalysts

To compare the efficiency of the active LDH catalyst, epoxidation of ethyl linoleate was performed over various other heterogeneous catalysts and the results are given in ESI Table S9. Table S9 also summarizes activity data of some of the reported catalysts. Commercial alumina catalysts were less active for this reaction. Under optimized conditions, highly basic MgAl and NiAl-LDHs showed lesser conversion than active $Co_{30}Cu_{70}$Al-LDH catalyst. Furthermore, substitution of copper by other divalent metal ions showed lesser selectivity for the epoxides (75-85%). These results augment the importance of redox properties present in CoCuAl-LDHs that play an important role in enabling this reaction.

Scale-up experiments

Scale-up studies (5-50 g) for sunflower oil indicated that the catalyst was active with 100% epoxide selectivity even at higher scale and the separation process became easier on higher scale. For 5&15 g scale, the conversions of sunflower oil were 67%, whereas at 50 g scale, the conversion was 60% with selectivity of diepoxide at 93, 83 and 83% respectively. Physical properties such as density, viscosity, oxygen content, oxidative stability and iodine number of neat and epoxidized sunflower oil were compared (Table 5). A decrease in the iodine number of the epoxidized sunflower oil confirmed the formation of oxirane ring. An increase in the oxygen content and viscosity (by nearly four times), and significant improvement in the oxidative stability by nearly four times for epoxidized sunflower oil than neat sunflower oil suggests their promise for them to be used in industrial applications.

Table 5 Comparison of the physical properties of neat and epoxidized sunflower oil

Properties	Sunflower oil	Epoxidized sunflower oil
Appearance	Light yellow	Golden yellow
Density (kg/m^3)	0.864	0.867
Viscosity at 40 °C (cP)	32.9	125.1
Oxygen content (%)[a]	10	33
Iodine number[b]	29.9	7.6
Oxidative stability[c]		
At 30 °C (years)	1.03	4.57
At 110 °C (hours)	5.6	52.5

[a]CHNS-O analysis; [b]Based on ^{1}H NMR analysis; [c]Rancimat analysis

Conclusions

CoCuAl-LDHs were synthesized with varying Co/Cu atomic ratios and characterized by various physicochemical techniques and studied for epoxidation of fatty derivatives. Among them, $Co_{30}Cu_{70}$Al-LDH showed a maximum conversion (85%) for ethyl linoleate with nearly stoichiometric selectivity (selectivity of mono and di epoxides were 13 and 87% respectively). Reasons for the enhanced activity of this catalyst was attributed to facile redox behavior and surface metal concentration as deduced from TPR and XPS studies respectively. The active catalyst was reusable up to six cycles without any significant change in the conversion. Selectively diepoxides for ethyl linoleate can be prepared by using the catalyst obtained by calcining $Co_{30}Cu_{70}$Al-LDH at 300 °C. Various vegetable oils (edible, non-edible and used cooking oils) were successfully epoxidized under the optimized conditions with moderate to good yields. It was revealed that the presence of glyceryl moiety in the oils could be the reason for reduced conversion to epoxides compared to ethyl linoleate/sunflower FAME, probably due to hindered access of the oxidant. Castor oil gave 98% monoepoxide selectivity although with lesser conversion (40%) suggests complete formation of ricinoleic epoxides. Removal of antioxidant and use of TBHP in decane further improved the conversion of oil. Scale-up on 50 g was successfully demonstrated for sunflower oil with similar yield of epoxide (as that of smaller scale). Significant improvement in the viscosity and oxidative stability of epoxidized oil suggest its promise for industrial applications.

Experimental section

Materials

The technical grade ethyl linoleate (assay ≥ 65%) was purchased from Fluka/Sigma-Aldrich and the vegetable oils

were purchased from local market. The ethyl linoleate had ~70% of linoleate and ~ 20% of oleate species. The acid value was determined by acid-base titration and the fatty acid compositions of vegetable oils were determined by GC-MS after converting them into fatty acid methyl esters (Shimadzu, QP 2010). Characteristic properties of the vegetable oils are given in ESI Table S10. TBHP (70 wt.% in water/95% in decane) were purchased from Sigma-Aldrich and toluene was purchased from SD fine chemicals, India.

Synthesis of LDH materials

LDH materials were synthesized by co-precipitation under low supersaturation method. A solution (A) containing the desired amount of metal nitrates (Co, Cu & Al) was mixed thoroughly to make a homogeneous solution, slowly (1 ml/min) and simultaneously mixed with a solution (B) containing precipitating agents (i.e., NaOH and Na_2CO_3) in a Schott autotitrator, at a constant pH of 9.5 ± 0.1 under vigorous stirring at room temperature. The addition took ~90 min and the final pH was adjusted to 10. In all the cases the ratio of divalent (Cu+Co) and trivalent (Al) metal ion was fixed as 3. The samples were aged in the mother-liquor at 65 °C for 18 h, filtered off, washed (until total absence of nitrates and sodium in the washing liquids) and dried in vacuum desiccator at room temperature for 48 h. The samples are named as CoxCuyAl-LDH, where 'x' and 'y' stands for the nominal atomic ratio of Co and Cu. As-synthesized samples were calcined in static air atmosphere for 5 h to obtain mixed metal oxides and are named as $Co_xCu_yAl\text{-}CLDH_T$ where 'T' is the calcination temperature.

Characterization techniques

Elemental analysis of the synthesized materials was carried out by inductively coupled plasma optical emission spectrometry (ICP-OES; Perkin Elmer Optima 2000 DV). Powder X-ray diffraction (PXRD) of the materials was carried out on a Rigaku Miniflex II system using Cu Kα radiation. The operating voltage and current were 30 kV and 15 mA, respectively. The step size was 0.04˚ with a step time of 0.2 s. Identification of the crystalline phases was made by comparing with the JCPDS files. FT-IR spectra were recorded in a Perkin-Elmer Spectrum-GX instrument, using KBr pellets; 100 scans were recorded with a nominal resolution of 4 cm^{-1}, which accumulated and averaged to improve the signal-to-noise ratio. FT-IR studies for TBHP treated LDH materials were performed by taking optimized amount of LDH (30 mg) and TBHP (1.4 ml) in a tightly packed centrifuge tube and was allowed to suspend well overnight. The partially-dried material was mixed with KBr and made as disc and was analyzed. For FT-IR analysis of liquid samples, chloroform was used as solvent

Thermogravimetric analysis (TGA) was done on Mettler Toledo instrument under a nitrogen atmosphere from 50 to 500 °C at a heating rate of 10 °C/min. Scanning electron microscopy (SEM) of the samples was analyzed in a microscope (Leo Series 1430 VP) equipped with EDX facility (Oxford Instruments). Analyses were carried out with an accelerating voltage of 20 kV and a working distance of 17 mm, with magnification values up to 100,000x. Acidic (or) basic strength of the catalysts was determined by the Hammett indicator method. The indicators namely benzalacetophenone (pKa = -5.6) and anthraquinone (pKa = -8.2) were used to determine acidic strength whereas methyl red (pKa = 5.1), neutral red (pKa = 6.8), phenolphthalein (pKa = 8.2), nile blue (pKa = 10.1) and tropaeolin O (pKa = 11) were used to determine basic strength. Temperature programmed reduction (TPR) of the samples was done using Autochem-2920 (Micromeritics). Samples were initially heated to 200 °C under nitrogen flow at a heating rate of 10 °C for 1 h and cooled to room temperature. TPR studies were then carried out by passing 2% H_2 in argon keeping the characteristic number K=100 by taking appropriate amount of material and by adjusting the flow rate of the gas[44] in the temperature range of 50-900 °C at a heating rate of 10 °C/min.

UV-vis spectra were recorded following the diffuse reflectance technique (UV-vis/DRS) on a Shimadzu UV-2550 using 5 nm slits and BaSO4 as reference. X-ray photoelectron spectroscopy (XPS) studies were carried out using AXIS Ultra 'DLD' X-ray photoelectron spectrometer built around the AXIS technology. Delay line detector was used for all the studies using Al-Kα radiation (1486.6 eV) as the excitation source with the pass energy of 40 eV. The vacuum during measurements was better than 5 × 10−8 mbar and data reduction and processing were performed using Kratos' Vision 2 processing software. The binding energy scale was calibrated with respect to the adventitious carbon (C 1s) at 284.6 eV. The error in the binding energy values in this study is ±0.1 eV. Specific surface area and pore size analysis of the samples were measured by nitrogen adsorption at -196 °C using a sorptometer (ASAP-2010, Micromeritics). The samples were degassed at 80 °C for 4 h prior to the measurements and the data were analyzed using published software. Small amount of liquid samples were diluted with tetrahydrofuran and Matrix Assisted Laser diffraction/ionization (MALDI-TOF) study was done in MALDI-TOF-Applied Biosystems (4800 Plus MALDI TOF/TOF analyzer) to find the mass of the compound. ^1H NMR analysis was done using Bruker Avance DPX 200 instrument with an operating frequency of 200 MHz. For each analysis 16 scans were recorded with a flip angle of 90º.

Epoxidation reaction

Technical grade ethyl linoleate was taken as a model compound for epoxidation reaction as most of the oils studied have nearly similar fatty acid compositions. Structurally vegetable oils have oleate/linoleate species that are attached with the glyceryl moieties. Epoxidation reactions were carried out in a 25 ml round-bottom flask fitted with a water cooled condenser. 1 g of ethyl linoleate/vegetable oil was mixed with 2 ml of toluene as solvent, and to that 30 mg of catalyst was added. 1.4 ml of TBHP was then added and kept in an oil bath at 110 °C for 4 h with vigorous stirring (1100 rpm). After the reaction, mixture was centrifuged to separate the catalyst. The organic layer was collected and excess toluene was evaporated under reduced pressure. The solvent free sample (15-30 µL) was dissolved in deutrated chloroform (500 µL) and analyzed by ^1H NMR using TMS as internal standard.

Conversion (%) was calculated based on the area of the protons appear at 2.01 ppm in ^1H NMR in both reactant and products. Selectivity (%) of mono and diepoxides were calculated based on the area of the protons appear at 2.9 and 3.1 ppm in ^1H NMR. In both the cases, the terminal methyl proton appears at 0.88 ppm was used as internal standard.[45] Duplicate experiments were conducted and average values are reporting here with an error of ± 2% for conversion and ±5% for epoxide selectivity. For scale-up studies, larger reactor vessels such as 250 ml or 1000 ml flask were used depending on the scale. Chemical shifts observed for vegetable oils and epoxidized oils

in ^{1}H NMR are given in ESI Fig. S17. Physical properties such as viscosity (Brookfield Viscometer; Model –LVOV-II+P), oxidative stability (Metrohm–873 Biodiesel Rancimat) and oxygen content (Perkin-Elmer CHNS/O analyzer; Series II, 2400) were analyzed for sunflower oil and epoxidized sunflower oil.

Acknowledgements

CSIR-CSMCRI Communication No. 034: Authors thank CSIR, New Delhi for financial support under Network Project NWP-010 (Inorganic materials for diverse applications). Authors thank "Analytical Discipline and Centralized Instrumental Facilities" for providing instrumentation facilities. Authors thank Kratos Analytical, UK and Perfomax Analytical, India for XPS measurements.

Notes and references

[a] Discipline of Inorganic Materials and Catalysis, CSIR-Central Salt and Marine Chemicals Research Institute (CSIR-CSMCRI), Council of Scientific and Industrial Research (CSIR), Gijubhai Badheka Marg, Bhavnagar- 364 002, (Gujarat), INDIA.

[b] Academy of Scientific and Innovative Research, CSIR-Central Salt and Marine Chemicals Research Institute (CSIR-CSMCRI), Council of Scientific and Industrial Research (CSIR), Gijubhai Badheka Marg, Bhavnagar- 364 002, (Gujarat), INDIA

Electronic Supplementary Information (ESI) available: [Physicochemical and surface properties of catalysts, TGA, SEM, UV-vis DRS and XPS of catalysts, time, temperature, stirring speed, nature of oxidant, catalyst amount and substrate:oxidant mole ratio variation studies over $Co_{30}Cu_{70}$Al-LDH, PXRD and FT-IR of calcined catalysts, activity of calcined catalysts and their reusability, PXRD, FT-IR and XPS of fresh and used catalysts, comparison of activity of various catalysts, characteristics of vegetable oils, MALDI-TOF of product, monitoring epoxidation with time using ^{1}H NMR spectra, epoxidation in presence of methyl oleate and *tert*-butanol, ^{1}H NMR chemical shifts for oleate and linoleate groups, schematic mechanism,]. See DOI: 10.1039/b000000x/

1 K. Motokura, D. Nishimura, K. Mori, T. Mizugaki, K. Ebitani, K. Kaneda, *J. Am. Chem. Soc.*, 2004, **126**, 5662.
2 A. Tsuji, K. T. V. Rao, S. Nishimura, A. Takagaki, K. Ebitani, *ChemSusChem*, 2011, **4**, 542.
3 S. Miyata, Clays and Clay Miner., 1983, **31**, 305.
4 A. Bissessur, M. Naicker. *Int. J. Phys. Sci.*, 2013, **8**, 1772.
5 D. Madhavan, K. Pitchumani, *Photochem. Photobiol., Sci.* 2003, **2**, 95.
6 Z.P. Xu, G.Q. (Max) Lu, *Pure Appl. Chem.*, 2006, **78**, 1771.
7 F. Cavani, F. Trifiro, A. Vaccari, *Catal. Today*, 1991, **11**, 173.
8 M.J. Climent, A. Corma, D.P. Frutos, S. Iborra, M. Noy, A. Velty, P. Concepción, *J. Catal.*, 2010, **269**, 140.
9 B. M. Choudary, M. L. Kantam, C. R. V. Reddy, K. K. Rao, F. Figueras, *J. Mol. Catal. A: Chem.*, 1999, **146**, 279.
10 U. Costantino, M. Curini, F. Montanari, M. Nocchetti, O. Rosati, *J. Mol. Catal. A: Chem.*, 2003, **195**, 245.
11 C. N. Pérez, C. A. Pérez, C. A. Henriques, J. L. F. Monteiro, *Appl. Catal. A: Gen.*, 2004, **272**, 229.
12 C. M. Jinesh, C. A. Antonyraj, S. Kannan, *Catal. Today*, 2009, **141**, 176.
13 S. Sankaranarayanan, C. A. Antonyraj, S. Kannan, *Bioresour. Technol.*, 2012, **109**, 57.
14 U. Biermann, U. Bornscheuer, M. A. R. Meier, J. O. Metzger, H. Schafer, *J. Angew. Chem. Int. Ed.*, 2011, **50**, 3854.
15 G. Du, A. Tekin, E. G. Hammond, L. K. Woo, *J. Am. Oil Chem. Soc.*, 2004, **81**, 477.
16 P. A. Z. Suarez, M. S. C. Pereira, K. M. Doll, B. K. Sharma, S. Z. Erhan, *Ind. Eng. Chem. Res.*, 2009, **48**, 3268.
17 A. Adhvaryu, S. Z. Erhan, *Ind. Crop. Prod.*, 2002, **15**, 247.
18 P. S. Lathi, B. Mattiasson, *Appl. Catal. B: Environ.*, 2007, **69**, 207.
19 S. C. Godoy, M. F. Ferrão, A. E. Gerbase, *J. Am. Oil Chem. Soc.*, 2007, **84**, 503.
20 Y. Guo, J. H. Hardesty, V. M. Mannari, J. L. Massingill Jr, *J. Am. Oil Chem. Soc.*, 2007, **84**, 929.
21 G. D. Yadav, D. V. Satoskar, *J. Am. Oil Chem. Soc.*, 1997, **74**, 397.
22 K. Lee, L. L. C. Wong, J. J. Blaker, J. M. Hodgkinson, A. Bismarck, *Green Chem.*, 2011, **13**, 3117.
23 V. V. Goud, A. V. Patwardhan, N. C. Pradhan, *Bioresour. Technol.*, 2006, **97**, 1365.
24 S. Dinda, A. V. Patwardhan, V. V. Goud, N. C. Pradhan, *Bioresour. Technol.*, 2008, **99**, 3737.
25 A. Campanella, M. A. Baltanas, M. C. Capel-Sanchez, J. M. Campos-Martin, J. L. G. Fierro, *Green Chem.*, 2004, **6**, 330.
26 M. Guidotti, N. Ravasio, R. Psaro, E. Gianotti, L. Marchese, S. Coluccia, *Green Chem.*, 2003, **5**, 421.
27 M. Guidotti, E. Gavrilova, A. Galarneau, B. Coq, R. Psaro, N. Ravasio, *Green Chem.*, 2011, **13**, 1806.
28 L. A. Rios, D. A. Echeverri, A. Franco, *Appl. Catal. A: Gen.*, 2011, **394**, 132.
29 M. Farias, M. Martinelli, D. P. Bottega, *Appl. Catal. A: Gen.*, 2010, **384**, 213.
30 M. Farias, M. Martinelli, G. K. Rolim, *Appl. Catal. A: Gen.*, 2011, **403**, 119.
31 J. K. Satyarthi, D. Srinivas, *Appl. Catal. A: Gen.*, 2011, **401**, 189.
32 S. Sun, G. Yang, Y. Bi, H. Liang, *J. Am. Oil Chem. Soc.*, 2011, **88**, 1567.
33 J. M. Fernandez, C. Barriga, M. A. Ulibarri, F. M. Labajos, V. Rives, *Chem. Mater.*, 1997, **9**, 312.
34 V. Rives, A. Dubey, S. Kannan, *Phys. Chem. Chem. Phys.*, 2001, **3**, 4826.
35 W. Ying, Q. Jiuhui, L. Huijuan, W. Rongcheng, *Chin. Sci. Bull.*, 2006, **51**, 1431.

36 A. Sinhamahapatra, P. Pal, A. Tarafdar, H.C. Bajaj, A. B. Panda, *ChemCatChem*, 2013, **5**, 331.
37 V. Rives, S. Kannan, *J. Mater. Chem.*, 2000, **10**, 489.
38 J. Carpentier, S. Siffert, J. F. Lamonier, *J. Porous Mater.*, 2007, **14**, 103.
39 D. G. Cantrell, L. J. Gillie, A. F. Lee, K. Wilson, *Appl. Catal. A: Gen.*, 2005, **287**, 183.
40 M. G. Vijayaraj, C. S. Gopinath, *J. Catal.*, 2006, **241**, 83.
41 S. Velu, K. Suzuki, C. S. Gopinath, H. Yoshida, T. Hattori, *Phys. Chem. Chem. Phys.*, 2002, **4**, 1990.
42 G. Fogassy, P. Ke, F. Figueras, P. Cassagnau, S. Rouzeau, V. Courault, G. Gelbard, C. Pinel, *Appl. Catal. A: Gen.*, 2011, **393**, 1.
43 Y. Miyake, K. Yokomizo, N. Matsuzaki, *J. Am. Oil Chem. Soc.*, 1997, 15.
44 D. A. M. Monti, A. Baiker, *J. Catal.*, 1983, **83**, 323.
45 H. A. J. Aerts, P. A. Jacobs, *J. Am. Oil Chem. Soc.*, 2004, **81**, 841.